Practical Papers, Articles and Application Notes

Flavio Canavero, Technical Editor

The first article of this issue belongs to the "Education Corner" series and represents an enlightening contribution on the spectral characteristics of digital signals. The article is entitled "Bandwidth of Digital Waveforms" and is authored by Professor Clayton R. Paul, who offers – with his usual clarity and rigor – a unified description of switching signals from the time- and frequency-domain point of view. He also points out a common misconception on the definition of bandwidth that is often employed in signal integrity applications.

The second article is entitled "EMI Failure Analysis Techniques, Part I on Frequency Spectrum Analysis" by Weifeng Pan and David Pommerenke from the EMC Lab of the Missouri University of Science and Technology in Rolla, Missouri. This paper is intended to be the first of a series covering different methods for EMI failure analysis of devices. This first contribution focuses on frequency-domain techniques and provides an interesting discussion of the use of spectrum analyzers.

In conclusion, I encourage (as always) all readers to actively participate to this column, either by submitting manuscripts they deem appropriate, or by nominating other authors having something exciting to share with the EMC community. I will follow all suggestions, and with the help of independent reviewers, I hope to be able to provide a great variety of enjoyable and instructive papers. Please communicate with me, preferably by email at canavero@ieee.org.

Bandwidth of Digital Waveforms

Clayton R. Paul, Mercer University, Macon, GA (USA), paul_cr@Mercer.edu

I. The Fourier Series and Periodic Waveforms

Waveforms of signals found in digital systems fall into two categories. The first are the periodic, deterministic waveforms such as clocks and similar timing signals. A *periodic* waveform $x(t)$ is one that repeats in intervals of length T where $T = {}^{1}/_{f_0}$ is the period in seconds which is the reciprocal of the fundamental repetition frequency of the waveform f_0, and t denotes time. In other words, $x(t) = x(t \pm kT)$ where $k = 1, 2, 3, \cdots$. Figure 1 shows a digital clock signal where the rise/fall times are denoted as τ_r and τ_f, respectively, and the pulse width τ is the time between the 50% levels. Realistic clock waveforms do not transition sharply as shown in Fig. 1 but smoothly transition at the beginning and end of the rise and fall time intervals. Hence it is common to state the rise/fall times as being between the 10% and 90% levels, and the relation between the rise/fall times of actual waveforms and the waveform in Fig. 1 is $\tau_{r,10-90\%} = 0.8\,\tau_r$.

The waveform of the deterministic, periodic digital clock waveform in Fig. 1 can *equivalently* be thought of as being the sum of a dc or average-value term and an *infinite sum* of sinusoids having frequencies that are integer multiples of the fundamental frequency, f_0, (harmonics) as [1]

$$\begin{aligned} x(t) &= c_0 + c_1\cos(\omega_0 t + \theta_1) + c_2\cos(2\omega_0 t + \theta_2) \\ &\quad + c_3\cos(3\omega_0 t + \theta_3) + \cdots \\ &= c_0 + \sum_{n=1}^{\infty} c_n\cos(n\omega_0 t + \theta_n) \end{aligned} \tag{1}$$

where $\omega_0 = 2\pi f_0$. This is one of many equivalent forms of the familiar Fourier series for a periodic waveform [2]. The constant (dc component) c_0 is the *average value* of the waveform over one period [1, 2]:

$$c_0 = \frac{1}{T}\int_0^T x(t)\,dt \tag{2a}$$

The magnitudes and angles of the sinusoidal components are computed from [1, 2]

$$c_n\angle\theta_n = \frac{2}{T}\int_0^T x(t)\,e^{-jn\omega_0 t}\,dt \tag{2b}$$

and $j = \sqrt{-1}$, $e^{-jn\omega_0 t} = \cos(n\omega_0 t) - j\sin(n\omega_0 t)$. For a single pulse or equivalently as $T \to \infty$, these discrete frequency components merge into a continuous spectrum which is called the Fourier transform of the single pulse.

For the digital clock spectrum shown in Fig. 1, a general expression can be obtained for the magnitudes and angles of the Fourier components in (1) and (2) but the result is somewhat complicated and little insight is gained from it [1]. However, if we restrict the result to trapezoidal pulses having equal rise/fall times, $\tau_r = \tau_f$, (which digital clock and data waveforms tend to approximate) we obtain a simple and informative result. For the case of equal rise and fall times we obtain [1]

$$c_0 = A\frac{\tau}{T}$$

$$c_n \angle \theta_n = 2A\frac{\tau}{T}\frac{\sin\left(\frac{n\pi\,\tau}{T}\right)}{\frac{n\pi\,\tau}{T}}\frac{\sin\left(\frac{n\pi\,\tau_r}{T}\right)}{\frac{n\pi\,\tau_r}{T}} \angle -n\pi\frac{(\tau+\tau_r)}{T}$$

$$\tau_r = \tau_f \tag{3}$$

This result is in the form of the product of two $\sin(x)/x$ expressions with the first depending on the ratio of the pulse width and the period, τ/T, (also called the *duty cycle* of the waveform, $D = \tau/T$) and the second depending on the ratio of the pulse rise/fall time and the period, τ_r/T. (The *magnitude* of the coefficient denoted as c_n must be a positive number. Hence there may be an additional $\pm 180^o$ added to the angle shown in (3) depending on the signs of each $\sin(x)$ term.) If, in addition to the rise and fall times being equal, the duty cycle is 50%, i.e. the pulse is "on" for half the period and "off" for the other half of the period, $\tau = 1/2\ T$, then the result for the coefficients given in (3) simplifies to

$$c_0 = \frac{A}{2}$$

$$c_n \angle \theta_n = A\frac{\sin\left(\frac{n\pi}{2}\right)}{\frac{n\pi}{2}}\frac{\sin\left(\frac{n\pi\,\tau_r}{T}\right)}{\frac{n\pi\,\tau_r}{T}} \angle -n\pi\left(\frac{1}{2}+\frac{\tau_r}{T}\right)$$

$$\tau_r = \tau_f,\ \tau = \frac{T}{2} \tag{4}$$

Note that the first $\sin(x)/x$ function is zero for n even so that for equal rise/fall times and a 50% duty cycle the even harmonics are (ideally) zero and the spectrum consists of only odd harmonics. By replacing n/T in (3) with the smooth frequency variable f, $n/T \rightarrow f$, we obtain the *envelope* of the magnitudes of the discrete frequencies as

$$c_n = 2A\frac{\tau}{T}\left|\frac{\sin(\pi f\tau)}{\pi f\tau}\right|\left|\frac{\sin(\pi f\tau_r)}{\pi f\tau_r}\right| \qquad \tau_r = \tau_f \tag{5}$$

In doing so, remember that the spectral components only occur at the discrete frequencies $f_0, 2f_0, 3f_0, \cdots$.

A *square wave* is the trapezoidal waveform where the rise/fall times are *zero*:

$$c_0 = A\frac{\tau}{T}$$

$$c_n \angle \theta_n = 2A\frac{\tau}{T}\frac{\sin\left(\frac{n\pi\,\tau}{T}\right)}{\frac{n\pi\,\tau}{T}} \angle -n\pi\frac{\tau}{T} \qquad \tau_r = \tau_f = 0 \tag{6}$$

Figure 2 shows a plot of the magnitudes of the c_n coefficients for a square wave where the rise and fall times are zero, $\tau_r = \tau_f = 0$. The envelope is shown with a dashed line. The spectral components appear only at *discrete* frequencies, $f_0, 2f_0, 3f_0, \cdots$. Observe that the envelope goes to zero where the argument of $\sin(\pi f\tau)$ goes to zero or $f = 1/\tau, 2/\tau, \cdots$.

Observe some important properties of the $\sin(x)/x$ function:

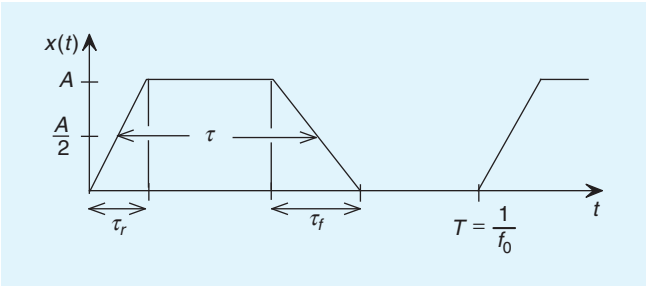

Fig. 1. A digital clock waveform.

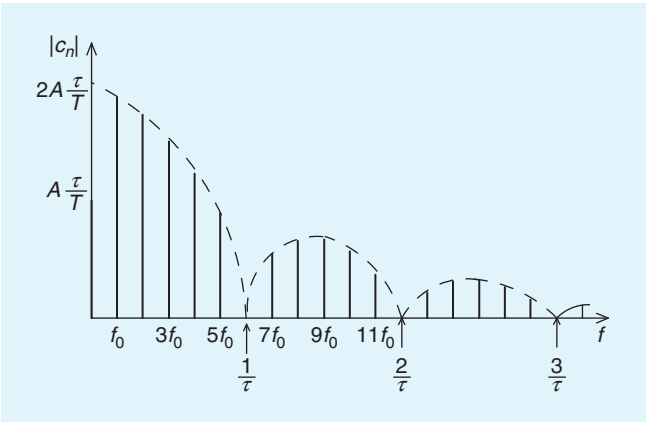

Fig. 2. Plot of the magnitudes of the c_n coefficients for a square wave, $\tau_r = \tau_f = 0$.

$$\lim_{x\to 0}\frac{\sin(x)}{x} = 1$$

which relies on the property that $\sin(x) \cong x$ for small x and

$$\left|\frac{\sin(x)}{x}\right| \le \begin{cases} 1 & x \le 1 \\ \frac{1}{x} & x \ge 1 \end{cases}$$

The second property allows us to obtain a *bound* on the magnitudes of the c_n coefficients and relies on the fact that $|\sin(x)| \le 1$ for all x. A more useful way of plotting the envelope of the magnitudes of the spectral coefficients is by plotting the horizontal frequency axis logarithmically and similarly plotting the magnitudes along the vertical axis in dB as $c_{n,\mathrm{dB}} = 20\log_{10}c_n$. The envelope as well as the bounds on the magnitudes of the coefficients for the $\sin(x)/x$ function are shown in Fig. 3. Observe that the actual result is bounded by 1 for $x \le 1$ and decreases at a rate of -20 dB/decade for $x \ge 1$. This rate is equivalent to a $1/x$ decrease. Also note that the magnitudes of the actual spectral components go to zero where the argument of $\sin(x)$ goes to zero or $x = \pi, 2\pi, 3\pi, \cdots$.

The amplitudes of the spectral components of a trapezoidal waveform where $\tau_r = \tau_f$ given in (3) are the product of two $\sin(x)/x$ functions: $\sin(x_1)/x_1 \times \sin(x_2)/x_2$. When log-log axes are used this gives the result for the bounds on the amplitudes of the spectral coefficients shown in Fig. 4. Note that the bounds are constant (0dB/decade) out to the first breakpoint where $f_1 = 1/\pi\,\tau = f_0/\pi\ D$. The *duty cycle* is $D = \tau/T = \tau\, f_0$. Above this they decrease at a rate of -20 dB/decade out to a second breakpoint of $f_2 = 1/\pi\,\tau_r$, and decrease at a rate of -40 dB/decade above that. The plot in Fig. 4 shows the

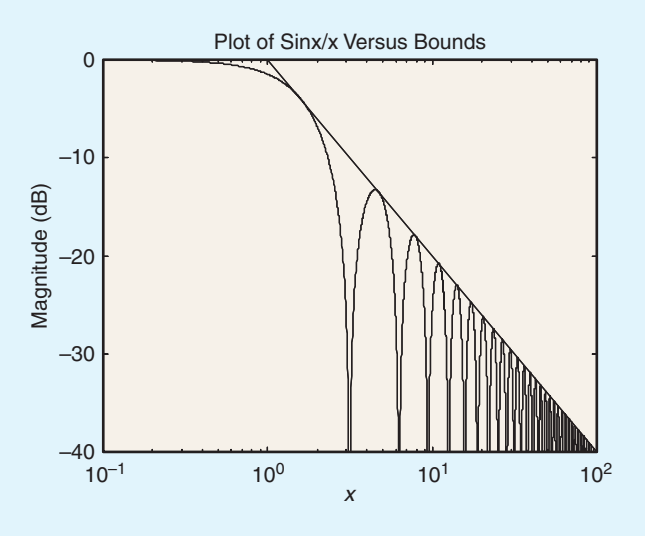

Fig. 3. The envelope and bounds of the $\sin(x)/x$ *function are plotted with logarithmic axes.*

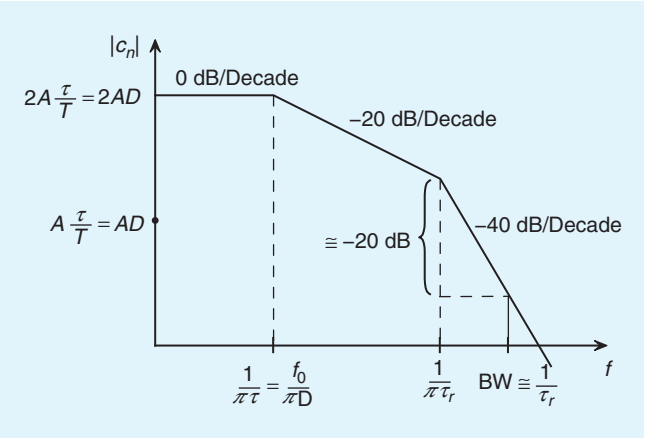

Fig. 4. Bounds on the clock waveform spectrum.

important result that *the spectral content of the waveform is determined by the pulse rise/fall times*. Longer rise/fall times push the second breakpoint lower in frequency thereby reducing the high-frequency spectral levels. Shorter rise/fall times push the second breakpoint higher in frequency thereby increasing the high-frequency spectral levels. A convenient and meaningful way of defining the bandwidth of a digital clock waveform (as we will show) is:

$$\mathrm{BW} \cong \frac{1}{\tau_r} \tag{7}$$

This amounts to going past the second breakpoint by a factor of approximately 3 thereby approximately cancelling the π in the denominator of the frequency of the second breakpoint. At this point, the bound on the spectrum is further reduced by approximately 20dB. Above this point the spectral magnitudes (their bound) are rolling off at -40 dB/decade and tend to become inconsequential.

The second type of waveforms are the trapezoidal digital data pulses where the period starts immediately after the previous pulse, i.e., $T = \tau + (\tau_r + \tau_f)/2$, but the occurrence of a pulse in these adjacent time intervals is random. The spectral content of these random waveforms is characterized in terms of the *power spectral density* which has a shape and properties similar to those for the deterministic waveform of Fig. 1 [1].

II. Determining the Error in a Reconstruction of the Waveform Using a Finite Number of Harmonics

Reconstruction of a waveform using the Fourier series in (1) ideally requires that we use an *infinite number* of harmonics. Since this is not possible, we use the first NH harmonics to give a finite-term approximation to the waveform

$$\tilde{x}(t) = c_0 + \sum_{n=1}^{\mathrm{NH}} c_n \cos(n\omega_0 \mathrm{t} + \theta_n) \tag{8}$$

It can be shown that the choice of the coefficients in (2) minimizes the Mean Square Error or MSE between the actual waveform and the finite-term approximation in (8):

$$\mathrm{MSE} = \frac{1}{T}\int_0^T [\mathrm{x}(t) - \tilde{\mathrm{x}}(t)]^2 \, \mathrm{d}t \tag{9}$$

This error criterion essentially adds the *point-wise errors* squared over a period and averages this over the period. It can be shown that adding successive harmonics will cause the approximate representation to converge uniformly to the true waveform in the mean-squared error sense. The MSE can be shown to give [1]

$$\mathrm{MSE} = \frac{1}{T}\int_0^T \mathrm{x}^2(t)\, \mathrm{d}t - c_0^2 - \sum_{n=1}^{\mathrm{NH}} \frac{c_n^2}{2} \tag{10}$$

For the trapezoidal waveform in Fig. 1 with equal rise/fall times, $\tau_r = \tau_f$, and a 50% duty cycle, the total average power in it is [1]

$$\begin{aligned} P_{av} &= \frac{1}{T}\int_0^T x^2(t)\, dt \\ &= A^2\left[\frac{1}{2} - \frac{1}{3}\frac{\tau_r}{T}\right] \quad \mathrm{W} \end{aligned} \tag{11}$$

The total average power in the finite-term approximation is

$$\begin{aligned} \tilde{P}_{av} &= \frac{1}{T}\int_0^T \tilde{x}^2(t)\, dt \\ &= c_0^2 + \sum_{n=1}^{\mathrm{NH}} \frac{c_n^2}{2} \end{aligned} \tag{12}$$

This simply means that *the average power in the approximation* $\tilde{x}(t)$ *is the sum of the average powers in the dc and harmonic terms* which is Parseval's theorem. So the usual choice of the coefficients of the Fourier series in (2) minimizes the difference in the total average powers in the waveforms. Note that the MSE seems to ignore errors in the angles of the coefficients, θ_n. However, the magnitudes and angles of the coefficients are related [2].

A more logical way of defining this representation error is the Mean Absolute Error or MAE:

$$\mathrm{MAE} = \frac{1}{T}\int_0^T |x(t) - \tilde{x}(t)|\, dt \qquad (13)$$

This absolute value weights a negative error, $\tilde{x} > x$, and a positive error, $x > \tilde{x}$, equally as it should. But the integral for the MAE in (13) cannot generally be integrated in closed form. Hence the alternative choice of the MSE in (9) is chosen simply to allow a closed form solution. In the remainder of this article we will numerically evaluate the MAE for a specific waveform.

We arbitrarily choose a 5 V, 1 GHz ($T = 1$ns) clock waveform having equal rise/fall times of $\tau_r = 100$ ps $= 0.1$ ns and a 50% duty cycle. Table 1 gives the magnitudes and angles of the coefficients for the first 13 harmonics. Note that the c_n coefficients (magnitude and angle) in (3) scale directly with the amplitude A and the ratios $D = \tau/T$ and τ_r/T. Hence the c_n coefficients of other waveforms having these same ratios can be obtained from those in Table 1. The wavelengths, $\lambda = v_0/f$, (in free space) for each harmonic are also given. Observe that the magnitudes of the harmonics tend to decrease with increasing frequency. Figure 5 shows the approximation of the finite-term approximation using the dc term and the first 3 harmonics along with the individual component waveforms. Figure 6 shows a similar comparison using the first 5 harmonics, and Fig. 7 shows the comparison using the first 9 harmonics. For this waveform the bandwidth according to the criterion in (7) is $\mathrm{BW} = 1/\tau_r = 10$ GHz. Hence, according to the criterion in (7), the BW consists of the first 9 harmonics, and the reconstruction of the waveform using 9 harmonics in Fig. 7 is quite good but the convergence for fewer numbers of terms is not as good.

Figures 8, 9, and 10 show the point-wise absolute error versus time, $|x(t) - \tilde{x}(t)|$, for various numbers of harmonics in a finite-term representation. While these plots of the point-wise absolute error are informative, we obtain a numerical value for the MAE in (13) using a trapezoidal numerical integration

TABLE 1. SPECTRAL (FREQUENCY) COMPONENTS OF A 5 V, 1 GHz, 50% DUTY CYCLE, 100 PS RISE/FALL TIME DIGITAL CLOCK SIGNAL.

Harmonic	f	λ	Level	Angle
1	1 GHz	30 cm	3.131 V	−108°
3	3 GHz	10 cm	0.9108 V	−144°
5	5 GHz	6 cm	0.4053 V	−180°
7	7 GHz	4.29 cm	0.1673 V	144°
9	9 GHz	3.33 cm	0.0387 V	108°
11	11 GHz	2.73 cm	0.0259 V	−108°
13	13 GHz	2.31 cm	0.0485 V	−144°

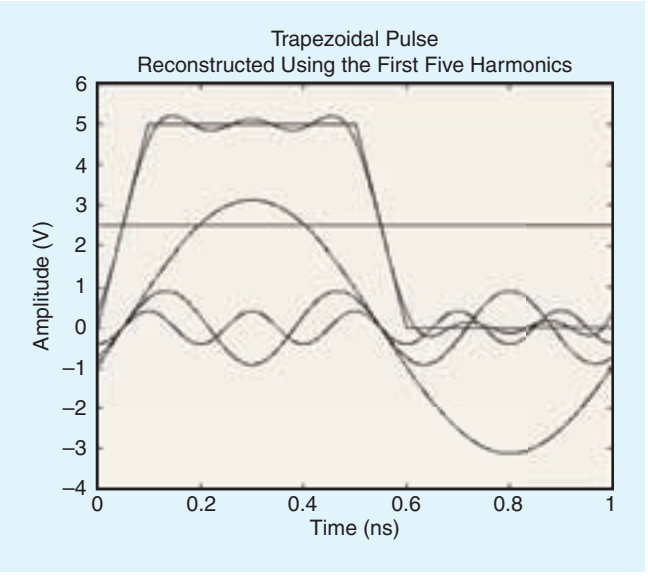

Fig. 6. Approximating the clock waveform using the first five harmonics.

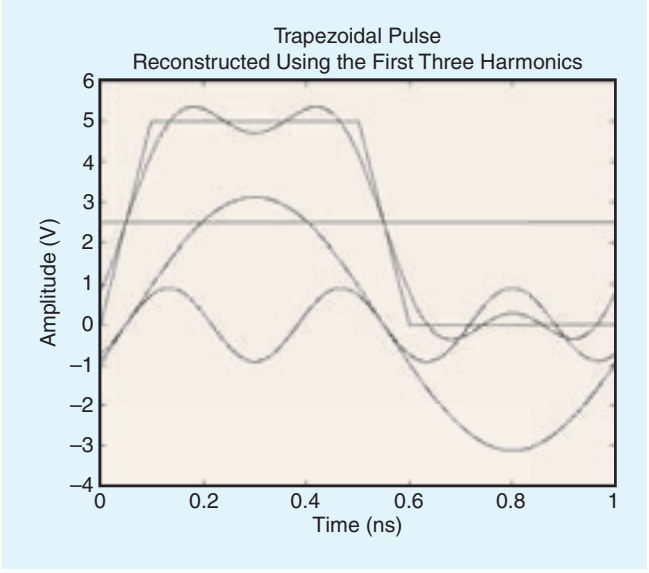

Fig. 5. Approximating the clock waveform with the first three harmonics.

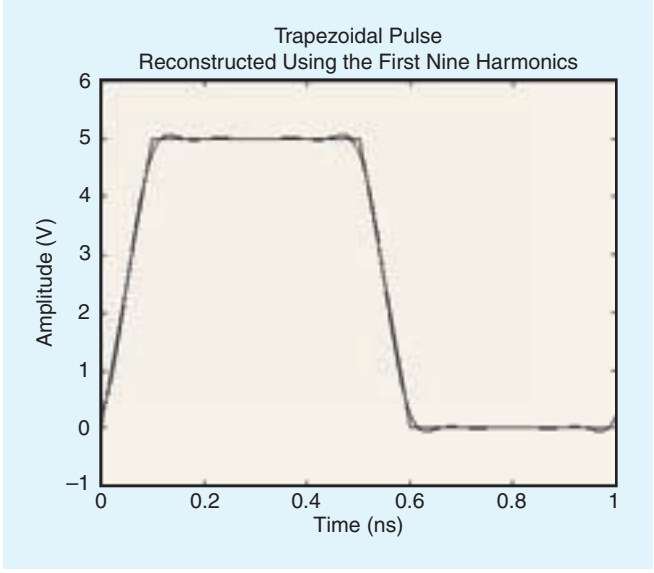

Fig. 7. Approximating the clock waveform using the first nine harmonics.

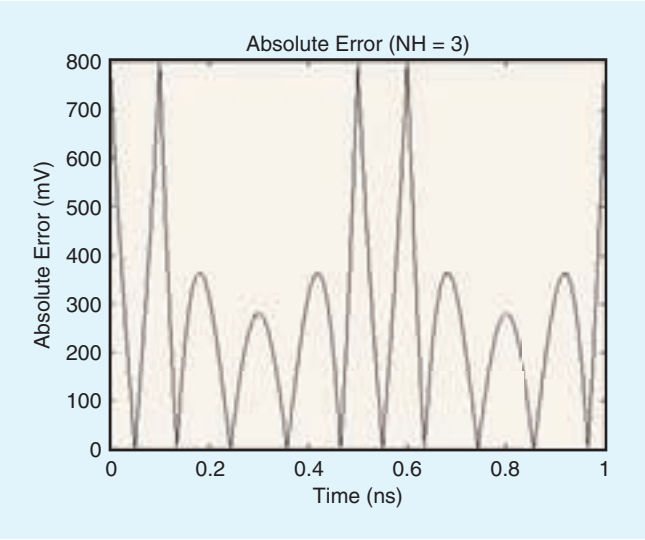

Fig. 8. Point-wise absolute error for 3 harmonics.

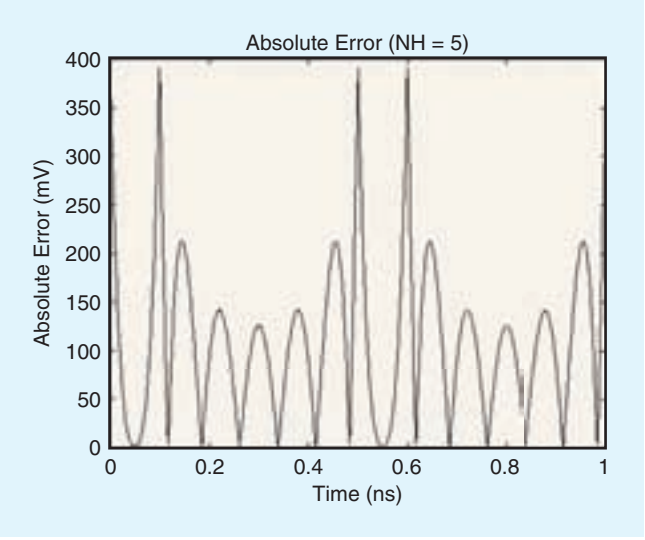

Fig. 9. Point-wise absolute error for 5 harmonics.

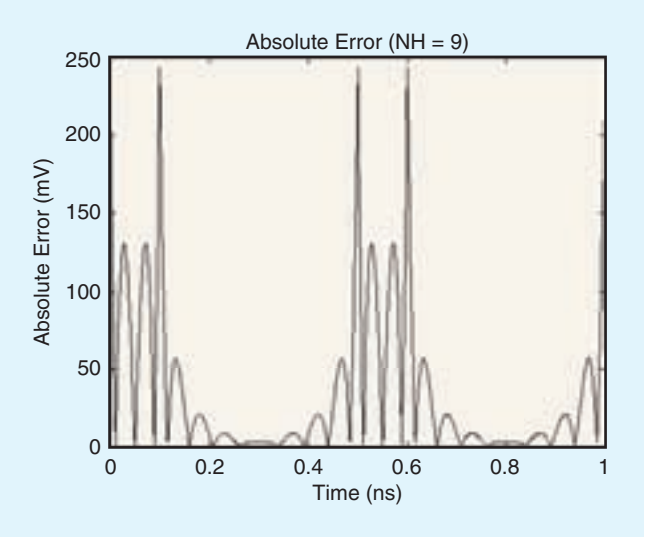

Fig. 10. Point-wise absolute error for 9 harmonics.

TABLE 2. MEAN ABSOLUTE ERROR FOR VARIOUS NUMBERS OF HARMONICS FOR A 5 V, 1 GHz, 0.1 NS RISE/FALL TIME, 50% DUTY CYCLE TRAPEZOIDAL WAVEFORM.

Number of Harmonics	Mean Absolute Error (mV)
1	600.3
3	265.2
5	110.1
7	50.2
9	35.0
11	39.3
13	33.0
15	22.1
17	15.5
19	12.2
21	13.9
23	12.8
25	9.9

routine. This gives the MAE in Table 2 for a large number of harmonics which is plotted in Fig. 11.

The criterion for the bandwidth given in (7) is somewhat arbitrary. The critical judge of its efficacy is how well a reconstructed signal using *only* a finite number of harmonics will approximate the signal. The criterion of MSE in (9) and (10) gives the reconstruction error in terms of the difference between the total average powers in the actual waveform and in its finite-term representation. For this digital clock waveform the total average power using (11) is 11.667 W. Using (12), the average power in the dc component is 6.25 W and the average powers in the first 13 harmonics are 4.9 W, 0.415 W, 82.1 mW, 14 mW, 0.75 mW, 0.335 mW, 1.18 mW. The total average power contained in the dc component and the first 9 harmonics is 11.663 W which is 99.97% of the total average power in the waveform. However, note that 96% of the total average power of the waveform is contained in the dc component and the first harmonic component! So the MSE is not a particularly discriminating criterion for the *significant spectral content of the waveform*. The MAE criterion in (13) gives a more relevant measure of the point-wise reconstruction error. Figure 11 gives an indication that the point-wise reconstruction error reaches a somewhat minimum level after about 9 harmonics which is the BW for this signal given in (7).

There are alternative measures of the BW that have been proposed. The most widely-used throughout the literature and trade magazines is

$$\mathrm{BW} = \frac{0.35}{\tau_{r,10-90\%}} = \frac{0.4375}{\tau_{r,0-100\%}} \qquad (14)$$

This gives a BW for the above 1 GHz waveform of 4.375 GHz thereby requiring only 3 harmonics for reconstruction of the original waveform. The results for only 3 harmonics shown in Figures 5, 8, and 11 show that this gives a relatively large point-wise error and hence a poor reconstruction of the clock waveform. Of particular importance is the point-wise error during the

steady-state region of the waveform where the waveform level should be the level A, i.e., during the "setup" and "hold" times. During this critical time, the point-wise error for NH = 3 is on the order of 300 mV, whereas the point-wise error for NH = 9 is on the order of 10 mV. *The BW criterion in (14) was derived in a fashion that has very little if anything to do with the bandwidth of a trapezoidal waveform*. So it is not surprising that it gives a poor approximation of the waveform particularly during the critical steady-state time interval. The derivation of this bandwidth criterion in (14) is as follows. A *square wave* is applied to the low-pass front end of an oscilloscope which is represented as an RC low-pass filter, and the problem is to determine the *resulting rise time* of the *output signal* (displayed on the face of the oscilloscope). Hence the BW criterion in (14) relates *the bandwidth of the RC filter*, $\mathrm{BW} = 1/(2\pi\mathrm{RC})$ to the *resulting rise time of the waveform that is displayed on the oscilloscope face*: the output of the filter. Hence the BW criterion in (14) is of questionable relevance for determining the BW of a trapezoidal waveform. We must avoid the temptation to use a formula such as (14) whose derivation or applicability is unknown solely because "it has the right words in it": in the case of (14) "bandwidth" and "rise time".

III. Transmission Lines and Signal Integrity

"Electrical lengths" of interconnect lines in *wavelengths*, λ, are more important than their "physical lengths" in meters. We say that a physical dimension is "electrically short" if it is no larger than approximately one-tenth of a wavelength [1]. *Interconnect lines that are electrically long cannot be analyzed using Kirchhoff's voltage and current laws and lumped-circuit analysis principles, and must be analyzed using the transmission line model*. For example, consider an interconnect line on a printed circuit board (PCB) having a velocity of propagation of $v = 1.7 \times 10^8$ m/s that carries a 1 GHz digital clock signal The wavelength of the fundamental frequency of 1 GHz on this PCB is $\lambda = v/f = 17$ cm (about 6.7 inches). Attempting to analyze an interconnect of length 1.7 cm (approximately 0.67 inches) using Kirchhoff's laws and lumped-circuit analysis principles will be valid for only the fundamental frequency of the waveform (1 GHz). Analysis for all higher harmonics will be considerably in error unless the line is modeled with the transmission-line model. This dilemma is becoming an increasing problem in today's high-speed and high-frequency digital and analog electronics whose interconnects carry signals having spectral content that today and in the near future is steadily moving into the GHz frequency range. *Thus the familiar lumped-circuit analysis methods are rapidly becoming obsolete, and transmission-line modeling of the interconnects is increasingly being required*!

To illustrate this, consider Fig. 12 which illustrates the connection of two CMOS buffers on a PCB. The PCB structure is a microstrip consisting of a land of width 10mils on one side of a glass-epoxy board ($\varepsilon_r = 4.7$) with a ground plane on the other side. The board thickness is 47 mils. This gives a characteristic impedance of the line of 124 ohms and a velocity of propagation of $v = 1.7 \times 10^8$ m/s [1]. The one-way time delay of the connection line is $T_D = L/v = 0.3$ ns where the length of the line is $L = 2$ inches = 5.08 cm. The source voltage $V_S(t)$ is a 5 V, 50 MHz trapezoidal waveform having a 50% duty cycle and various rise/fall times. The output impedance of the first buffer is represented by 10 Ω, and the input to the second buffer is represented by a 5 pF capacitance, all of which are typical for CMOS devices although the actual output impedance is somewhat nonlinear.

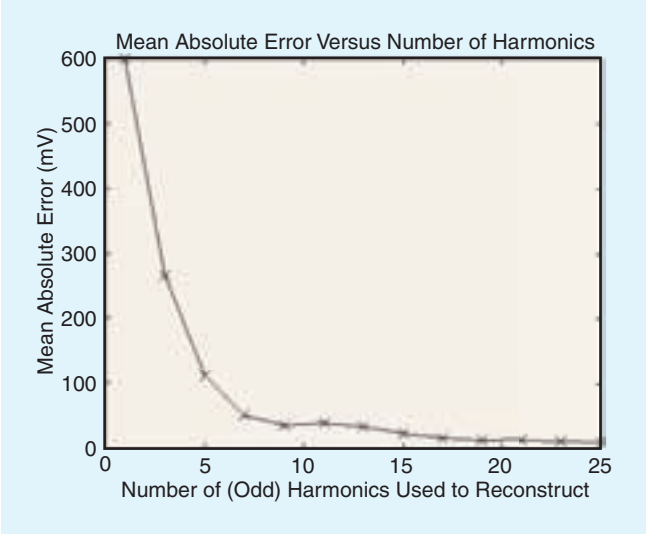

Fig. 11. Plot of the MAE for various numbers of harmonics used to reconstruct the waveform.

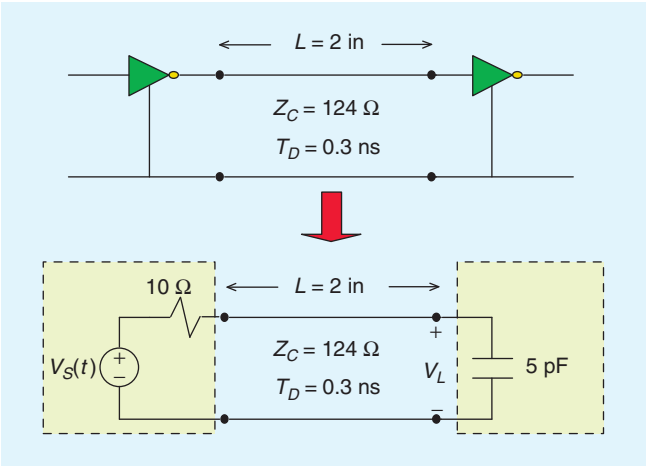

Fig. 12. Illustration of signal integrity problems associated with fast rise/fall times.

If the connection line is "electrically short" at the *highest significant frequency of the source waveform* (the BW) then we expect that the line will have little effect on the transmission of the signal from the source to the load other than imposing the inevitable time delay of $T_D = 0.3$ ns. The line is electrically short at the highest significant frequency of the signal being carried by the line conductors if

$$L < \frac{1}{10}\lambda = \frac{1}{10}\frac{v}{f_{\max}} \tag{15}$$

This can be written in terms of the one-way time delay as

$$f_{\max} < \frac{1}{10L}v = \frac{1}{10T_{\mathrm{D}}} \tag{16}$$

The line in Fig. 12 is electrically short at 333 MHz. Using the criterion for the BW of $V_S(t)$ in (7), $f_{\max} = \mathrm{BW} = 1/\tau_r$, leads to the criterion for the line to be electrically short at the highest significant frequency of $V_S(t)$ and therefore to not significantly effect the signal transmission as

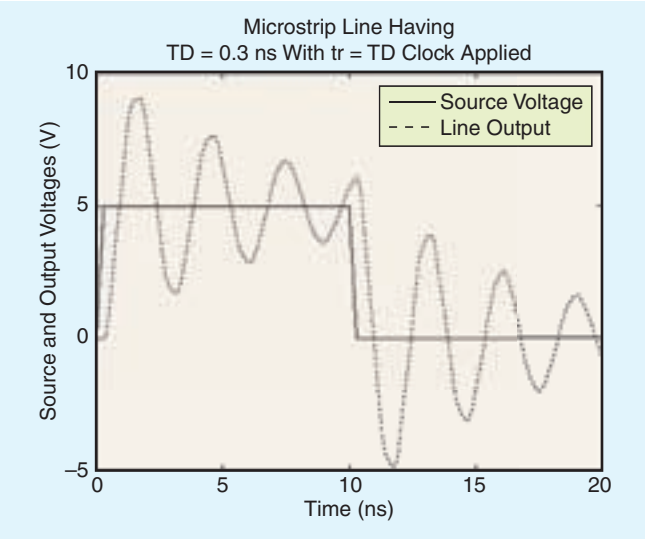

Fig. 13. Comparison of the output and source (clock) waveforms for a transmission line having a time delay of 0.3 ns *and a clock signal having* $\tau_r = T_D = 0.3$ ns.

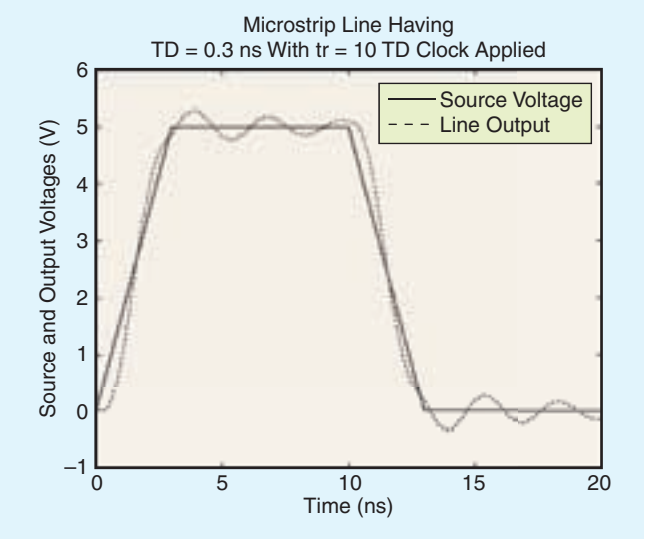

Fig. 14. Comparison of the output and source (clock) waveforms for a transmission line having a time delay of 0.3 ns *and a clock signal having* $\tau_r = 10T_D = 3$ ns.

$$\tau_r > 10\ T_D \tag{17}$$

The remaining figures illustrate this relationship and were obtained using the exact transmission-line model of the line contained in PSPICE [1]. Figure 13 shows that for a clock signal having a frequency of 50 MHz $(T = 20$ ns$)$ and $\tau_r = T_D = 0.3$ ns there is significant "ringing" on the load voltage resulting in logic errors. Since the line is electrically short at 333 MHz and the bandwidth of $V_S(t)$ is BW $= 1/\tau_r = 3.33$ GHz, the line is electrically long for a significant portion of the spectrum of $V_S(t)$ and this is expected. Figure 14 shows that for the criterion in (17), $\tau_r = 10T_D = 3$ ns, having a bandwidth of BW $= 1/\tau_r = 333$ MHz, the line is electrically short for the significant frequencies of $V_S(t)$, and there is an insignificant ringing. Using the criterion in (14) for the BW $= 0.4375/\tau_r$, (17) becomes $\tau_r > 4.375T_D = 1.313$ ns. Figure 15 shows that for this rise time there is significant ringing on the load voltage

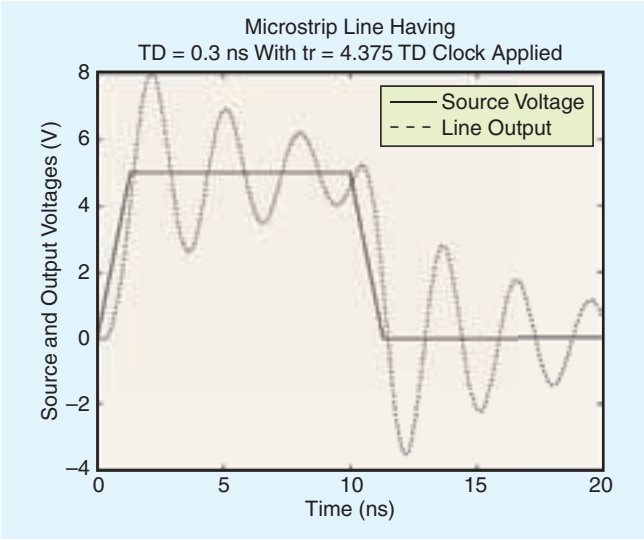

Fig. 15. Comparison of the output and source (clock) waveforms for a transmission line having a time delay of 0.3 ns *and a clock signal having* $\tau_r = 4.375T_D = 1.313$ ns.

waveform again demonstrating that the bandwidth criterion in (14) is an inadequate measure of the bandwidth of the input signal for the purposes of determining signal integrity.

IV. Summary

The bandwidth of a signal waveform should logically be defined as the minimum number of harmonic terms required to reconstruct the original periodic waveform such that adding more harmonics gives a negligible gain in the reduction of the point-wise reconstruction error, whereas using less harmonics gives an excessive point-wise reconstruction error. This article has suggested that choosing the bandwidth of a digital clock signal as being the inverse of the rise/fall time of the waveform gives a reasonable (and easily-remembered) criterion for the spectral content of that signal which achieves these objectives. The computed data for a specific but representative digital clock waveform support this choice for the BW although this choice is still somewhat arbitrary. However, an engineer must in the end weigh his/her constraints in choosing the necessary bandwidth criterion

References

[1] C.R. Paul, *Introduction to Electromagnetic Compatibility*, 2nd edition, John Wiley Interscience, Hoboken, NJ, 2006.

[2] C.R. Paul, *Essential Math Skills for Engineers*, John Wiley, Hoboken, NJ, 2009.

Biography

Clayton R. Paul *received the B.S. degree, from The Citadel, Charleston, SC, in 1963, the M.S. degree, from Georgia Institute of Technology, Atlanta, GA, in 1964, and the Ph.D. degree, from Purdue University, Lafayette, IN, in 1970, all in Electrical Engineering. He is an Emeritus Professor of Electrical Engineering at the University of Kentucky*

where he was a member of the faculty in the Department of Electrical Engineering for 27 years retiring in 1998. Since 1998 he has been the Sam Nunn Eminent Professor of Aerospace Systems Engineering and a Professor of Electrical and Computer Engineering in the Department of Electrical and Computer Engineering at Mercer University in Macon, GA. He has published numerous papers on the results of his research in the Electromagnetic Compatibility (EMC) of electronic systems and given numerous invited presentations. He has also published 16 textbooks and Chapters in four handbooks. Dr. Paul is a Life Fellow of the Institute of Electrical and Electronics Engineers (IEEE) and is an Honorary Life Member of the IEEE EMC Society. He was awarded the IEEE Electromagnetics Award in 2005 and the IEEE Undergraduate Teaching Award in 2007. **EMC**